Cancer Immunol Immunother (2011) 60:1801–1810
DOI 10.1007/s00262-011-1082-7

ORIGINAL ARTICLE

H_2O_2 production within tumor microenvironment inversely correlated with infiltration of $CD56^{dim}$ NK cells in gastric and esophageal cancer: possible mechanisms of NK cell dysfunction

Shinichirou Izawa · Koji Kono · Kousaku Mimura · Yoshihiko Kawaguchi · Mitsuaki Watanabe · Takanori Maruyama · Hideki Fujii

Received: 28 December 2010 / Accepted: 19 July 2011 / Published online: 3 August 2011

Abstract Human NK cells can be divided into two subsets, $CD56^{dim}CD16(+)$NK and $CD56^{bright}CD16(-)$NK cells, based on their expression of CD56 and CD16. In the present study, we analyzed the relationship between $CD56^{dim}$/$CD56^{bright}$ NK cells and H_2O_2 in tumor-infiltrating NK cells in patients with gastric ($n = 50$) and esophageal ($n = 35$) cancer. The ratio of $CD56^{dim}$ NK cells infiltrating tumors gradually decreased according to disease progression. H_2O_2 was abundantly produced within tumor microenvironments, and there was an inverse correlation between $CD56^{dim}$ NK cell infiltration and H_2O_2 production. $CD56^{dim}$ NK cells are more sensitive to apoptosis induced by physiological levels of H_2O_2 than $CD56^{bright}$ NK cells. Furthermore, the exposure of NK cells to H_2O_2 resulted in the impairment of ADCC activity. In conclusion, H_2O_2 produced within tumor microenvironments inversely correlated with the infiltration of $CD56^{dim}$ NK cells, possibly due to their preferentially induced cell death. These observations may explain one of the mechanisms behind NK cell dysfunction frequently observed in tumor microenvironments.

Keywords NK cells · CD16 · CD56 · Gastric cancer · Esophageal cancer · H_2O_2

Introduction

Therapeutic monoclonal antibodies (mAbs) such as Trastuzumab and Cetuximab targeting the HER family constitute a novel and attractive approach to treat cancer [1–3], and antibody-dependent cellular cytotoxicity (ADCC) was proven to be one of the important mechanisms of therapeutic mAbs [4, 5]. However, we and others have reported that Trastuzumab- and Cetuximab-mediated ADCC is impaired in comparison with healthy donors due to NK cell dysfunction [6–8]. In general, NK cell dysfunction has been reported in various types of malignancy, including an imbalance in their activating and inhibitory receptor repertoire such as NKG2D and CD161 [9], low expression of the signal transducing ζ chain on NK cells [10, 11], and the down-regulation of cytotoxic machinery on NK cells caused by immunosuppressive cytokines such as IL-10 and TGF-beta [12, 13]. Thus, improvement of the NK cell function may result in the resolution of impaired ADCC in patients with cancer, leading to successful treatment with Trastuzumab and Cetuximab.

Human NK cells can be divided into two subsets, $CD56^{dim}CD16(+)$NK and $CD56^{bright}CD16(-)$NK cells, based on their expression of CD56 and CD16 [14]. It has been thought that $CD56^{dim}$ NK cells are potent cytotoxic cells which mainly mediate ADCC, while $CD56^{bright}$ NK cells produce high levels of cytokines such as IFN-γ and regulate the immune response [14], although the biological relationship between $CD56^{dim}$ and $CD56^{bright}$ NK cells is still unclear. Regarding the relationship between $CD56^{bright}$ and $CD56^{dim}$ NK cells, it has been reported that an increased ratio of $CD56^{bright}$-to-$CD56^{dim}$ NK cells was observed in the presence of a chronic inflammatory status, such as rheumatoid arthritis and tuberculosis [15]. Moreover, these observations might be explained by the fact that $CD56^{bright}$ NK cells are more resistant to reactive oxygen species (ROS)-induced apoptosis than $CD56^{dim}$ NK cells, and ROS are abundantly produced at chronic inflammatory sites [16, 17]. However, with regard to $CD56^{dim}$ and

S. Izawa · K. Kono (✉) · K. Mimura · Y. Kawaguchi · M. Watanabe · T. Maruyama · H. Fujii
First Department of Surgery, University of Yamanashi, 1110 Shimokato, Chuo-city, Yamanashi 409-3898, Japan
e-mail: kojikono@yamanashi.ac.jp

$CD56^{bright}$ NK cells in tumor-bearing hosts, the preferential apoptosis of $CD56^{dim}$ NK cells was observed in patients with head and neck and breast cancer [18], but very limited information was provided. Thus, these observations prompted us to investigate the relationship between $CD56^{bright}$ and $CD56^{dim}$ NK cells within tumor microenvironments, in order to clarify the mechanisms behind NK cell dysfunction.

In the present study, we analyzed the relationship between $CD56^{dim}$/$CD56^{bright}$ NK cells and ROS in tumor-infiltrating NK cells in gastric and esophageal cancer patients.

Materials and methods

Patients

Fifty patients with gastric cancer (37 men and 13 women) and 35 patients with esophageal squamous cell carcinoma (ESCC) (32 men and 3 women), who were operated on in the University of Yamanashi Hospital from May 2009 to May 2010, were enrolled in the present study. The characteristics of the patients are shown in Table 1.

Patients with gastric cancer were divided into 2 groups: those with early disease ($n = 32$) corresponding to stage I according to the TNM classification for gastric cancer (UICC. 6th edition), and those with advanced disease corresponding to stage II, III, and IV ($n = 18$). Patients with ESCC were divided into 2 groups: those with early disease ($n = 10$) corresponding to stage 0 and stage I of the TNM classification for esophageal cancer (UICC. 6th edition), and those with advanced disease corresponding to stage II, III, and IV ($n = 25$).

Blood samples were taken from 20 healthy volunteers (18 men and 2 women; 38.1 ± 10.1 years). This study was approved by the ethics committee of the University of Yamanashi, and written informed consent was obtained from all patients.

Table 1 Characteristics of the patients

	Gastric cancer ($n = 50$)	Esophageal cancer ($n = 35$)
Age (years old)		
Total	67.7 ± 10.8	66.8 ± 8.26
Early disease	69.5 ± 9.51 ($n = 32$)	67.3 ± 4.5 ($n = 10$)
Advanced disease	64.4 ± 12.4 ($n = 18$)	66.7 ± 9.6 ($n = 25$)
Stage 0	–	3
Stage I	32	7
Stage II	6	11
Stage III	9	10
Stage IV	3	4
T1	30	14
T2	7	5
T3	11	15
T4	2	1
N0	29	15
N1	19	20
N2	2	ND
N3	–	ND

TNM classification of gastric and esophageal cancer (6th edition, UICC)

Chemicals and cell lines

Human catalase was purchased from GE Health Care (Uppsala, Sweden), and H_2O_2 was purchased from Sigma-Aldrich (St. Louis, MO, USA). Anti-HER2 mAb Trastuzumab (Herceptin, Roche, Basel, Switzerland) and anti-CD20 mAb Rituxan (Roche), which is an isotype-matched control mAb, were used for the antibody-dependent cell-mediated cytotoxicity assay (ADCC).

The esophageal squamous cell carcinoma (ESCC) cell line TE4 was a kind gift from Dr. Nishihara (Institute of Development, Aging and Cancer, University of Tohoku, Sendai, JAPAN).

Cell preparation and NK purification

PBMCs were isolated using Ficoll-Paque Plus (Amersham Biosciences, Uppsala, Sweden) density gradient solution. Tumor tissue and normal mucosa were isolated during surgery and homogenized by mechanical mincing with X-VIVO15 medium (CAMBREX, East Rutherford, NJ, USA). Subsequently, the single-cell suspension was purified by centrifugation with Ficoll-Paque Plus. Cells derived from peripheral blood, tumor tissue, and normal mucosa were subjected to subsequent assay on fresh cells without cryopreservation or any digestion step. After the cell preparation, the viability of PBMCs, tumor-infiltrating lymphocytes, and intraepithelial lymphocytes (IELs) were >95%, 75–90%, and 75–85%, respectively. Although some artifactual components such as dead cells might be contaminated, these components were removed in the analysis by gate-out with flow cytometry.

To prepare NK cells by negative selection, the NK cells were isolated from PBMCs by centrifugation with Ficoll-Paque after being incubated with the RosetteSep antibody cocktail for NK cells (StemCell Technologies Inc., Vancouver, British Columbia, Canada). The RosetteSep antibody cocktail was bound in bispecific antibody complexes, which are directed against cell surface antigens on human hematopoietic cells (CD3, CD4, CD19, CD36, and CD66b) and glycophorin A on red blood cells. Unwanted cells,

which adhered to red blood cells, and desired cells were separated using a Ficoll-Paque density gradient. The purified cells were confirmed to be more than 93% positive for CD56(+)CD3(−)NK cells by flow cytometry.

Immunohistochemistry

8-hydroxy-2′-deoxyguanosine (8OHdG) staining was conducted using the avidin–biotin-peroxidase complex method (Vectastain ABC elite kit, Vector laboratories, Burlingame, CA, USA) [18]. Briefly, each paraffin section was dewaxed, followed by antigen retrieval with target retrieval solution (10 mmol citrate buffer (pH 6.0), DAKO) with an autoclave (121°C, 15 min), and sections were incubated for 20 min with diluted normal blocking serum. Then, anti-8OHdG-monoclonal-antibody (the Japan Institute for the Control of Aging, Fukuroi, Japan) was applied for 4 h at room temperature. Thereafter, the sections were incubated with 1% H_2O_2 for 10 min, and peroxidase-linked secondary antibodies and diaminobenzidine were used to detect specific binding. The sections were counterstained with hematoxylin. The 8OHdG positive cells in tumor tissue were expressed as the mean values in five randomly selected areas at 400 × magnification.

Flow cytometry

For the distribution of $CD56^{dim}$ and $CD56^{bright}$ NK cells, lymphocytes were stained with CD16-FITC, CD56-PE, and CD3-APC (DAKO, Glostrup, Denmark), and $CD56^{dim}$CD16(+)NK or $CD56^{bright}$CD16(−)NK cells gated on CD56(+)CD3(−) cells were expressed as a percentage of the total NK cells (CD56(+)CD3(−) cells) (Fig. 1a).

For the apoptosis assay, apoptosis in each cell was measured by staining with FITC-conjugated Annexin V and 7AAD (MBL, Nagoya, Japan) following the manufacturer's recommendations.

H_2O_2 production assay with flow cytometry

The production of hydrogen peroxide (H_2O_2) by both baseline and stimulated monocytes was assessed by the formation of intracellular 2′,7′-dichlorofluorescein (DCF) [20]. Cells in 200 µl of X-VIVO were incubated with 5 µl of 1 mM 5-chloromethyl-2′,7′-dichlorodihydrofluorescein diacetate, acethyl ester (CM-H2DCFDA; Invitrogen, OR, USA) for 20 min at 37°C in a shaking water bath shielded from light in the presence or absence of phorbol myristate acetate (PMA; Wako, Japan; final concentration: 0.5 µg/ml). The reaction was stopped by the addition of 100 µl of ice-cold PBS, and cells were stained with CD14-APC (Dako). The production of H_2O_2 was determined as: mean DCF fluorescence intensity of PMA-stimulated CD14(+) cells—mean DCF fluorescence intensity of non-stimulated CD14(+) cells. *Tert*-butyl hydroperoxide (TBHP, 100 µM, Molecular Probes, OR, USA) was used as a positive control.

Antibody-dependent cell-mediated cytotoxicity assay by NK cells

After the target cells (HER2-overexpressing ESCC, TE4) were labeled with 50 µCi of ^{51}Cr for 60 min, target cells (5×10^3/well) and purified NK cells were co-incubated at various effector/target ratios in 200 µl of X-VIVO medium in a 96-well U-bottomed plate in triplicate with Trastuzumab (5 µg/ml) or the control mAb, Rituxan (5 µg/ml). After 6 h of incubation, the radioactivity of the supernatant (100 µl) was measured with a γ-counter. The percentage of specific lysis was determined as: 100 × (experimental cpm − spontaneous cpm)/(maximum cpm − spontaneous cpm).

Statistical analysis

The paired Student's *t*-test was used to examine differences between the IELs and TILs. The non-paired Student's *t*-test was used to examine differences between the advanced and early disease. Correlations between values were evaluated using non-parametric Spearman's rank correlation. Findings were considered significant when *P* values were <0.05.

Results

Distribution of $CD56^{dim}$ and $CD56^{bright}$ NK cells in tumor-infiltrating NK cells in patients with gastric and esophageal cancer

Representative flow cytometric data of CD16/CD56/CD3 staining for PBLs and TILs were shown in Fig. 1a. $CD56^{dim}$CD16(+)NK or $CD56^{bright}$CD16(−)NK cells gated on CD56(+)CD3(−)NK cells were expressed as a percentage of the total NK cells (Fig. 1b). In the patients with gastric cancer ($n = 50$), the decreased ratio of $CD56^{dim}$ NK to $CD56^{bright}$ NK cells was significant in TILs compared to intraepithelial lymphocytes (IELs) of the normal gastric mucosa (Fig. 1b). Furthermore, the decreased ratio of $CD56^{dim}$ NK cells in TILs was more pronounced in advanced ($n = 18$) rather than early disease ($n = 32$) of gastric cancer. Similarly, a significantly decreased ratio of $CD56^{dim}$ NK cells was observed in TILs of esophageal cancer ($n = 35$) compared to IELs of the normal esophageal mucosa, and the level of the decrease in $CD56^{dim}$ NK cells in TILs was more pronounced in advanced ($n = 25$) than in early disease of esophageal cancer ($n = 10$) (Fig. 1b).

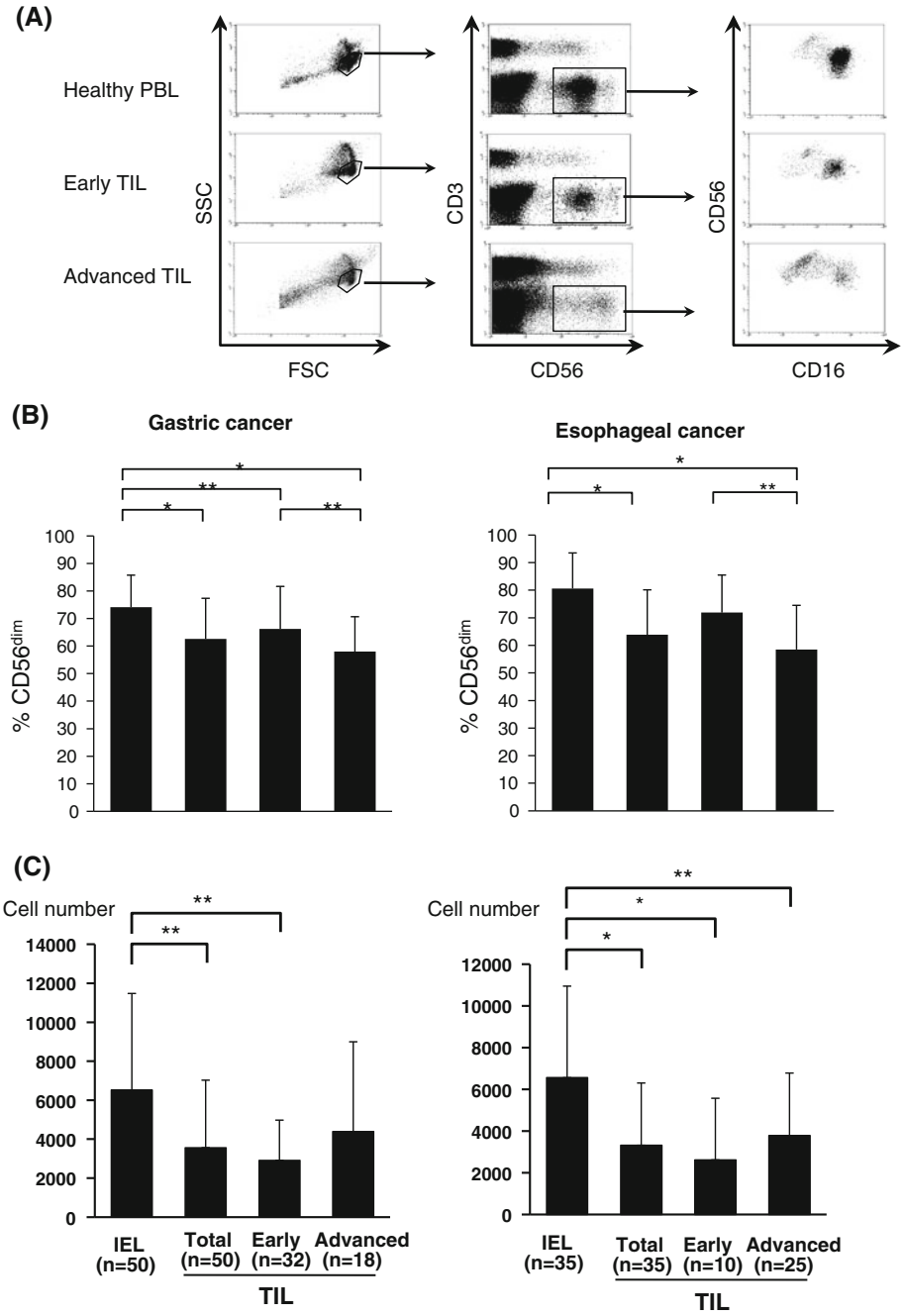

Fig. 1 Ratio of $CD56^{dim}CD16(+)$NK cells in tumor-infiltrating NK cells. Lymphocytes were stained with CD16-FITC, CD56-PE, and CD3-APC. Representative flow cytometric data of tumor-infiltrating lymphocytes (TIL) from early disease (Early) and advanced disease (Advanced) gastric cancer as well as peripheral blood lymphocytes (PBL) from healthy donors are shown in (**a**). The ratio of $CD56^{dim}CD16(+)$NK cells (%$CD56^{dim}$) is expressed as the percentage of total NK cells in TILs from early disease (Early) and advanced disease (Advanced) gastric cancer (**b**) and esophageal cancer (**b**) in comparison with those in intraepithelial lymphocytes (IELs) of the normal mucosa. The absolute number of $CD56^{dim}CD16(+)$NK cells per 5 mm^3 tissue sample is expressed in TILs from early disease (Early) and advanced disease (Advanced) gastric cancer (**c**) and esophageal cancer (**c**) in comparison with those in intraepithelial lymphocytes (IELs) of the normal mucosa. *$P < 0.01$, **$P < 0.05$

Furthermore, when the absolute number of $CD56^{dim}$ NK cells per 5 mm^3 tissue samples was calculated, decreased number of $CD56^{dim}$ NK cells were observed in TILs in comparison with IELs in both gastric and esophageal cancer (Fig. 1c).

On the contrary, there was no significant difference in the distribution of $CD56^{dim}$ NK cells in PBMCs between cancer patients and healthy donors (94.7 ± 2.8% in health donors, 93.6 ± 6.2% in gastric cancer, and 95.1 ± 3.5% in ESCC).

Thus, regarding the tumor microenvironment, the infiltrating ratio of $CD56^{dim}$ NK cells and the absolute number of $CD56^{dim}$ NK cells was significantly decreased in comparison with the normal mucosa and their levels of infiltrating ratio gradually decreased according to disease progression.

H_2O_2 production within tumor microenvironments

Since it was shown that $CD56^{dim}$ NK cells are more sensitive to ROS than $CD56^{bright}$ NK cells [17], we evaluated the levels of H_2O_2 within tumor microenvironments employing immunohistochemical analysis with 8OHdG staining [19]

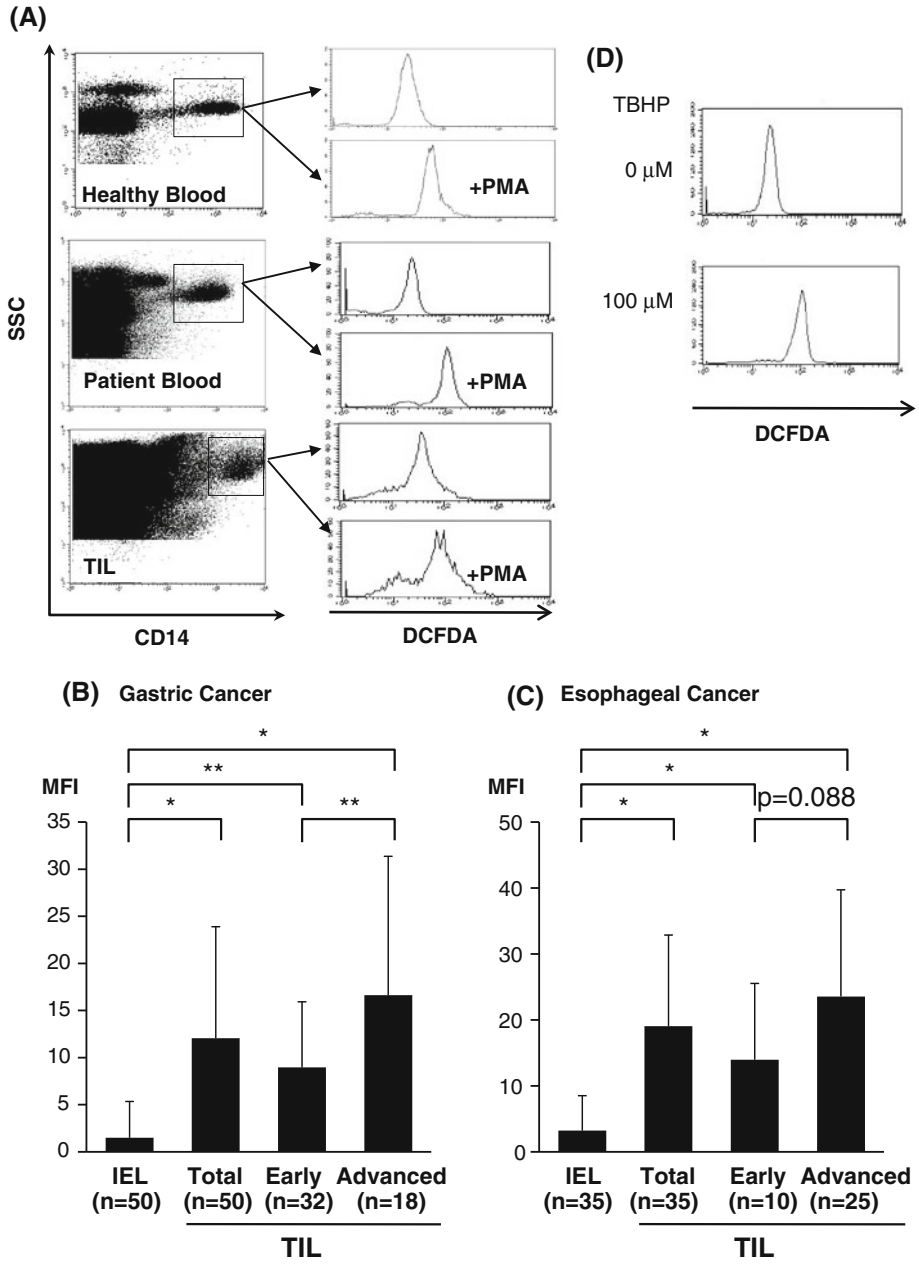

Fig. 2 H_2O_2 production of tumor-infiltrating macrophages. The production of hydrogen peroxide (H_2O_2) by CD14(+) cells was assessed by flow cytometry based on the formation of intracellular 2′,7′-dichlorofluorescein (DCF). Representative flow cytometric data (**a**) show that H_2O_2 was determined as: the mean fluorescence intensity (MFI) of PMA-stimulated CD14(+) cells—MFI of non-stimulated CD14(+) cells. Summarized data from tumor-infiltrating macrophages in early disease (Early) and advanced disease (Advanced) gastric (**b**) and esophageal (**c**) cancer in comparison with those in intraepithelial lymphocytes (IELs) of the normal mucosa are shown. Representative flow cytometric data for a positive control are shown using tumor-infiltrating macrophages in the presence of *Tert*-butyl hydroperoxide (TBHP) (**d**). $^*P < 0.01$, $^{**}P < 0.05$, *MFI* mean fluorescence intensity

and flow cytometric analysis with the DCFDA/PE-CD14 technique [20].

As shown in Fig. 2a, the production of H_2O_2 from tumor-infiltrating Mϕ can be evaluated quantitatively by flow cytometry. As a result, H_2O_2 production was significantly elevated in TILs in comparison with IELs of the normal gastric mucosa, and the level of H_2O_2 production within TILs was more pronounced in advanced than in early disease of gastric cancer (Fig. 2b). Similarly, H_2O_2 production was significantly increased in TILs in comparison with IELs of the normal esophageal mucosa, and the level of H_2O_2 production within TILs was more pronounced in advanced than in early disease of ESCC (Fig. 2c). Thus, the level of H_2O_2 production in TILs was up-regulated according to disease progression (Fig. 2b and c).

In order to confirm the quantitative accuracy regarding the grade of H_2O_2 by flow cytometry, immunohistochemical (IHC) staining with anti-8OHdG mAb was semiquantitatively performed for the same cohorts. Representative staining for 8OHdG as well as CD56 in the serial section is shown in Fig. 3a. The grade of 8OHdG-positive cells with IHC in TILs was significantly correlated with the levels of H_2O_2 production of tumor-infiltrating Mϕ with flow cytometry in each patient with gastric cancer and ESCC (Fig. 3b and c). Taken together, these observations strongly indicate that H_2O_2 was abundantly

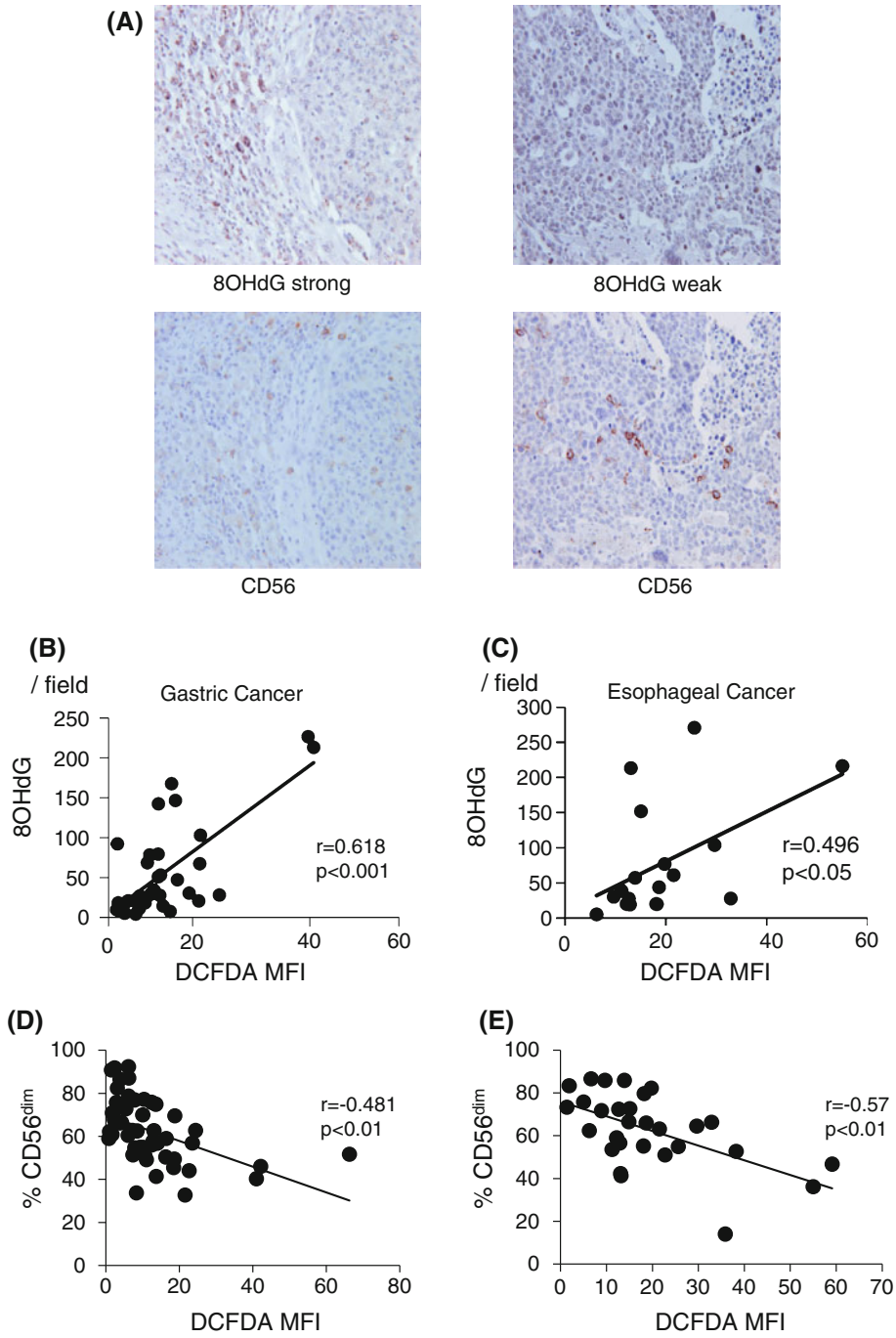

Fig. 3 Correlation between $CD56^{dim}$ NK cell infiltration and H_2O_2 production within tumor microenvironments. IHC staining with anti-8OHdG mAb was semiquantitatively performed for gastric ($n = 50$) and esophageal ($n = 35$) cancer. Representative staining for 8OHdG and CD56 in the serial sections is shown in (**a**). The grade of 8OHdG-positive cells in TILs was significantly correlated with the levels of H_2O_2 production of tumor-infiltrating Mϕ with flow cytometry in each patient with gastric cancer (**b**) and ESCC (**c**). When each value of $CD56^{dim}$ NK cell infiltration and H_2O_2 production in individual cases was plotted in gastric cancer ($n = 50$) and ESCC ($n = 35$), there were significant inverse correlations between $CD56^{dim}$ NK infiltration and H_2O_2 production within tumor microenvironments. *MFI* mean fluorescence intensity

produced within tumor microenvironments, and the levels of H_2O_2 were up-regulated according to disease progression.

Correlation between $CD56^{dim}$ NK infiltration and H_2O_2 production within tumor microenvironments

When each value of $CD56^{dim}$ NK infiltration and H_2O_2 production in individual cases was plotted in gastric cancer and ESCC (Fig. 3d and e), there were significant inverse correlations between $CD56^{dim}$ NK infiltration and H_2O_2 production within tumor microenvironments.

Apoptosis of NK cells after treatment with H_2O_2

Purified NK cells with negative selection from PBMCs of healthy donors ($n = 9$) were incubated with H_2O_2 for 4 h at the indicated doses of physiological levels and were subjected to apoptosis analysis with 7AAD- and Annexin V staining in combination with CD56/CD16 mAbs. Representative flow

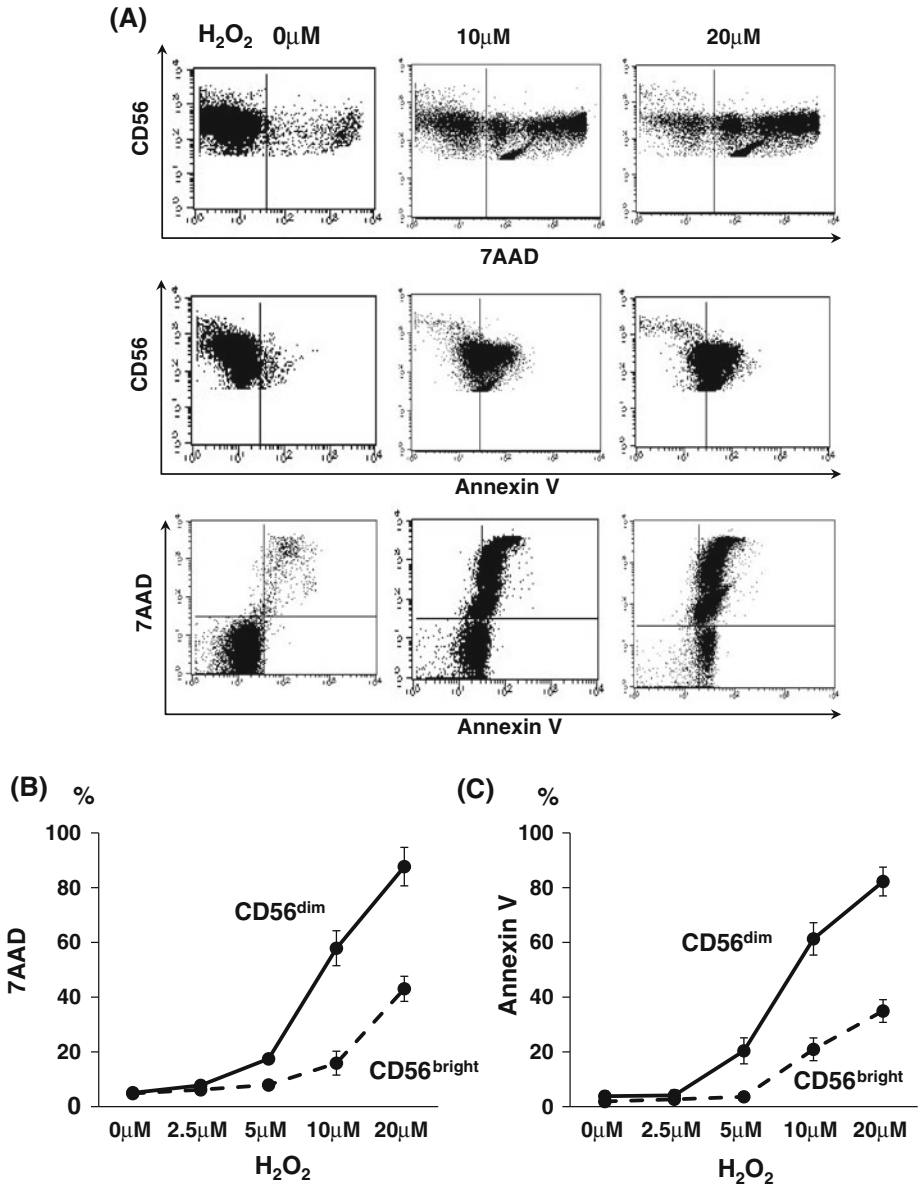

Fig. 4 Apoptosis of NK cells after treatment with H_2O_2. Purified NK cells were incubated with H_2O_2 for 4 h at indicated doses within physiological levels and were subjected to apoptosis analysis with 7AAD and FITC-conjugated Annexin V staining in combination with CD56/CD16 mAbs. Representative flow cytometric data for $CD56^{dim}$ NK cells indicated that $CD56^{dim}$ NK cells underwent apoptosis on exposure to H_2O_2 in a dose-dependent manner (**a**). Of note, there were marked differences in the grade of apoptosis between $CD56^{dim}$ NK and $CD56^{bright}$ NK cells (**b** and **c**). These observations were confirmed in 9 independent experiments using PBMCs from different donors

cytometric data for $CD56^{dim}$ NK cells indicated that $CD56^{dim}$ NK cells underwent apoptosis with exposure to H_2O_2 in a dose-dependent manner (Fig. 4a). Of note, there were marked differences in the grade of apoptosis between $CD56^{dim}$ NK and $CD56^{bright}$ NK cells (Fig. 4b). These observations were confirmed in 6 independent experiments using PBMCs from different donors. Thus, $CD56^{dim}$ NK cells are more sensitive to apoptosis induced by H_2O_2 than $CD56^{bright}$ NK cells.

NK dysfunction after treatment with H_2O_2

In order to evaluate the functional consequence of NK cell exposure to H_2O_2, purified NK cells from healthy donors (5A) and gastric cancer patients (5B) were treated with H_2O_2 for 4 h in combination with catalase, which is a selective inhibitor of H_2O_2, and subjected to Trastuzumab-mediated ADCC assays for HER2-overexpressing ESCC, TE4, in which the number of treated NK cells was adjusted as effector cells just before ADCC assays.

As shown in Fig. 5a, purified NK cells efficiently killed TE4 cells by Trastuzumab-mediated ADCC, with 87% lysis at a 20:1 of E/T ratio. When the purified NK cells were treated with H_2O_2, Trastuzumab-mediated ADCC was markedly down-regulated to 68% (10 μM) and 17% (20 μM) lysis, respectively, and the decreased ADCC was completely restored by the addition of catalase (Fig. 5a). Representative ADCC data from different experiments clearly showed that the down-regulation of ADCC induced by H_2O_2 was dose-dependent (Fig. 5c). These observations

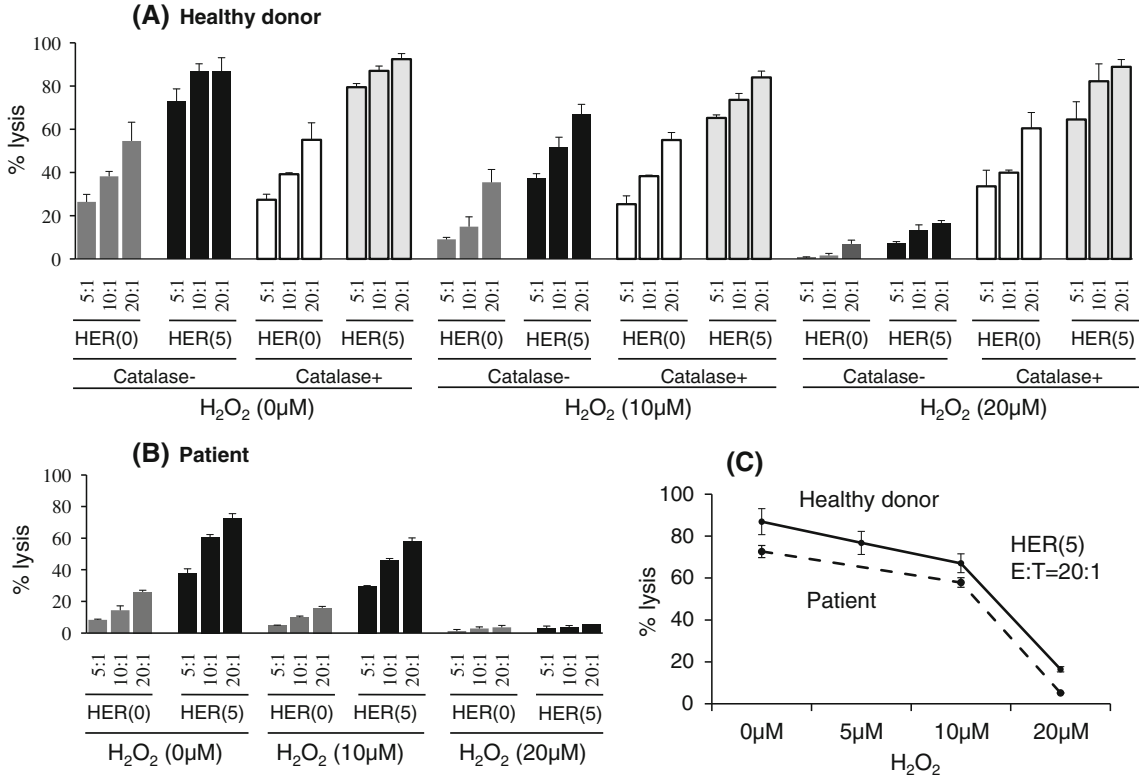

Fig. 5 NK dysfunction after treatment with H_2O_2. Purified NK cells were treated with H_2O_2 for 4 h in combination with catalase and subjected to Trastuzumab-mediated ADCC assays for HER2-overexpressing ESCC, TE4, in which the number of treated NK cells was adjusted as effector cells just before ADCC assays. Representative data of ADCC assay are shown in PBLs from a healthy donor (**a**) and a gastric cancer patient (**b**). These observations were confirmed in 6 independent experiments using PBMCs from the healthy donors and 4 independent experiments using PBMCs from the patients. Representative ADCC data from different experiments clearly showed that the down-regulation of ADCC induced by H_2O_2 was dose-dependent (**c**). *HER* Herceptin (Trastuzumab), *E/T* effector/target ratio

were confirmed in 6 independent experiments using PBMCs from different donors. Thus, with exposure to H_2O_2, NK cells exhibited impaired ADCC activity.

Discussion

The present study provided novel and clinically important findings relevant to the relationship between NK cell infiltration and H_2O_2 within the tumor microenvironments of gastric and esophageal cancer. First, the infiltrating ratio of $CD56^{dim}$ NK cells within the tumor gradually decreased according to disease progression. Second, H_2O_2 was abundantly produced within tumor microenvironments, and there was an inverse correlation between $CD56^{dim}$ NK cell infiltration and H_2O_2 production. Third, $CD56^{dim}$ NK cells are more sensitive to apoptosis in the presence of physiological levels of H_2O_2 than $CD56^{bright}$ NK cells. Furthermore, with exposure to H_2O_2, NK cells showed impaired ADCC activity.

In general, the grade of tumor-infiltrating NK cells correlates with better prognosis in patients with various cancers [21, 22]. Furthermore, it has been shown that not only the number of tumor-infiltrating NK cells, but also the per cell expression of CD16 in tumor-infiltrating NK cells correlates with the functional capacity of NK cells in cancer patients [23]. In the present study, we presented novel findings that the infiltrating ratio of $CD56^{dim}$ NK cells gradually decreased according to the disease progression of tumors. Taken together, both the infiltrating grade and characteristic difference in tumor-infiltrating NK cells are involved in the regulation of NK-mediated immunity within tumor microenvironments.

As one of the mechanisms behind the infiltrating ratio of $CD56^{dim}$ NK cells gradually decreasing with disease progression, we showed in the present study that $CD56^{dim}$ NK cells are more sensitive to apoptosis induced by H_2O_2 within tumors than $CD56^{bright}$ NK cells. These observations are consistent with a previous report that exposure to H_2O_2 of $CD56^{dim}$ NK cells resulted in the lost expression of cytotoxic function-related receptors such as NKp46 and NKG2D and then selectively undergo cell death in comparison with $CD56^{bright}$ NK cells [17]. In addition, it was shown that $CD56^{dim}$ NK cells in tuberculosis patients were

more susceptible to apoptosis than $CD56^{bright}$ NK cells [15]. These observations support our finding that H_2O_2 produced within tumor microenvironments induced the preferential cell death of $CD56^{dim}$ NK cells, leading to an inverse correlation of $CD56^{dim}$ NK cell infiltration with H_2O_2 production. To explain the difference in the sensitivity to H_2O_2 between $CD56^{bright}$ NK and $CD56^{dim}$ NK cells, it has been reported that $CD56^{bright}$ NK cells have more increased intracellular anti-oxidative functions such as involving paraoxonase-2 and lysozyme, which were up-regulated at least sixfold in $CD56^{bright}$ NK compared to $CD56^{dim}$ NK cells [24–26].

Reactive oxygen species (ROS) such as H_2O_2 are produced by activated granulocytes and Mϕ during inflammation [27, 28] and also by tumor cells [29, 30]. In the present study, we confirmed that H_2O_2 was abundantly produced within tumor microenvironments of gastric and esophageal cancer using both flow cytometry and IHC, and H_2O_2 production gradually increased according to disease progression. As it has been shown that the biology of human cancer may reflect chronic or recurrent inflammation [31], it is possible that H_2O_2 production may reflect the grade of inflammation within tumors. The local cytokine or chemokine milieu relating to inflammation could activate tumor-infiltrating Mϕ or granulocytes, leading to H_2O_2 production within tumors.

The concept that H_2O_2 produced within a tumor induces preferential cell death of $CD56^{dim}$ NK cells in the present study may explain why NK cell dysfunction is frequently observed in tumor microenvironments [32–34]. However, it has been reported that H_2O_2 exhibits both apoptotic and stimulatory effects on T cells [35, 36]. Thus, there may be dose windows of H_2O_2 regarding its action on T and NK cells. Alternatively, other unknown factors in addition to H_2O_2 may be involved in the regulation of apoptotic signals in NK cells.

In conclusion, there was an inverse correlation between $CD56^{dim}$ NK cell infiltration and H_2O_2 production in the tumor microenvironments of gastric and esophageal cancer, and H_2O_2 could induce the preferential cell death of $CD56^{dim}$ NK cells. A better understanding of immunoregulation relating to H_2O_2 production may lead to the improvement of NK cell functions within tumor microenvironments.

Conflict of interest The authors have no conflicts of interest.

References

1. Slamon DJ, Leyland-Jones B, Shak S, Fuchs H, Paton V, Bajamonde A, Fleming T, Eiermann W, Wolter J, Pegram M, Baselga J, Norton L (2001) Use of chemotherapy plus a monoclonal antibody against HER2 for metastatic breast cancer that overexpresses HER2. N Engl J Med 344:783–792
2. Cunningham D, Humblet Y, Siena S, Khayat D, Bleiberg H, Santoro A, Bets D, Mueser M, Harstrick A, Verslype C, Van Chau I, Cutsem E (2004) Cetuximab monotherapy and cetuximab plus irinotecan in irinotecan-refractory metastatic colorectal cancer. N Engl J Med 351:337–345
3. Hall PS, Cameron DA (2009) Current perspective—trastuzumab. Eur J Cancer 45:12–18
4. Zhang W, Gordon M, Schultheis AM, Yang DY, Nagashima F, Azuma M, Chang HM, Borucka E, Lurje G, Sherrod AE, Iqbal S, Groshen S, Lenz HJ (2007) FCGR2A and FCGR3A polymorphisms associated with clinical outcome of epidermal growth factor receptor expressing metastatic colorectal cancer patients treated with single-agent cetuximab. J Clin Oncol 25:3712–3718
5. Musolino A, Naldi N, Bortesi B, Pezzuolo D, Capelletti M, Missale G, Laccabue D, Zerbini A, Camisa R, Bisagni G, Neri TM, Ardizzoni A (2008) Immunoglobulin G fragment C receptor polymorphisms and clinical efficacy of trastuzumab-based therapy in patients with HER-2/neu-positive metastatic breast cancer. J Clin Oncol 26:1789–1796
6. Mimura K, Kono K, Hanawa M, Kanzaki M, Nakao A, Ooi A, Fujii H (2005) Trastuzumab-mediated antibody-dependent cellular cytotoxicity against esophageal squamous cell carcinoma. Clin Cancer Res 11:4898–4904
7. Kawaguchi Y, Kono K, Mimura K, Sugai H, Akaike H, Fujii H (2007) Cetuximab induce antibody-dependent cellular cytotoxicity against EGFR-expressing esophageal squamous cell carcinoma. Int J Cancer 120:781–787
8. Kono K, Takahashi A, Ichihara F, Sugai H, Fujii H, Matsumoto Y (2002) Impaired antibody-dependent cellular cytotoxicity mediated by herceptin in patients with gastric cancer. Cancer Res 62:5813–5817
9. Konjevic G, Mirjacic Martinovic K, Vuletic A, Jovic V, Jurisic V, Babovic N, Spuzic I (2007) Low expression of CD161 and NKG2D activating NK receptor is associated with impaired NK cell cytotoxicity in metastatic melanoma patients. Clin Exp Metastasis 24:1–11
10. Kono K, Salazar-Onfray F, Petersson M, Hansson J, Masucci G, Wasserman K, Nakazawa T, Anderson P, Kiessling R (1996) Hydrogen peroxide secreted by tumor-derived macrophages down-modulates signal-transducing zeta molecules and inhibits tumor-specific T cell-and natural killer cell-mediated cytotoxicity. Eur J Immunol 26:1308–1313
11. Kono K, Ressing ME, Brandt RM, Melief CJ, Potkul RK, Andersson B, Petersson M, Kast WM, Kiessling R (1996) Decreased expression of signal-transducing zeta chain in peripheral T cells and natural killer cells in patients with cervical cancer. Clin Cancer Res 2:1825–1828
12. Tsuruma T, Yagihashi A, Hirata K, Torigoe T, Araya J, Watanabe N, Sato N (1999) Interleukin-10 reduces natural killer (NK) sensitivity of tumor cells by downregulating NK target structure expression. Cell Immunol 198:103–110
13. Lee JC, Lee KM, Kim DW, Heo DS (2004) Elevated TGF-beta1 secretion and down-modulation of NKG2D underlies impaired NK cytotoxicity in cancer patients. J Immunol 172:7335–7340
14. Cooper MA, Fehniger TA, Caligiuri MA (2001) The biology of human natural killer-cell subsets. Trends Immunol 22:633–640
15. Schierloh P, Yokobori N, Aleman M, Musella RM, Beigier-Bompadre M, Saab MA, Alves L, Abbate E, de la Barrera SS, Sasiain MC (2005) Increased susceptibility to apoptosis of CD56dimCD16+ NK cells induces the enrichment of IFN-gamma-producing CD56bright cells in tuberculous pleurisy. J Immunol 175:6852–6860
16. Batoni G, Esin S, Favilli F, Pardini M, Bottai D, Maisetta G, Florio W, Campa M (2005) Human CD56bright and CD56dim natural killer cell subsets respond differentially to direct stimulation with

Mycobacterium bovis bacillus Calmette-Guerin. Scand J Immunol 62:498–506
17. Harlin H, Hanson M, Johansson CC, Sakurai D, Poschke I, Norell H, Malmberg KJ, Kiessling R (2007) The CD16- CD56(bright) NK cell subset is resistant to reactive oxygen species produced by activated granulocytes and has higher antioxidative capacity than the CD16+ CD56(dim) subset. J Immunol 179:4513–4519
18. Bauernhofer T, Kuss I, Henderson B, Baum AS, Whiteside TL (2003) Preferential apoptosis of CD56dim natural killer cell subset in patients with cancer. Eur J Immunol 33:119–124
19. Kondo S, Toyokuni S, Iwasa Y, Tanaka T, Onodera H, Hiai H, Imamura M (1999) Persistent oxidative stress in human colorectal carcinoma, but not in adenoma. Free Radic Biol Med 27:401–410
20. Takahashi A, Kono K, Ichihara F, Sugai H, Amemiya H, Iizuka H, Fujii H, Matsumoto Y (2003) Macrophages in tumor-draining lymph node with different characteristics induce T-cell apoptosis in patients with advanced stage-gastric cancer. Int J Cancer 104:393–399
21. Coca S, Perez-Piqueras J, Martinez D, Colmenarejo A, Saez MA, Vallejo C, Martos JA, Moreno M (1997) The prognostic significance of intratumoral natural killer cells in patients with colorectal carcinoma. Cancer 79:2320–2328
22. Ishigami S, Natsugoe S, Tokuda K, Nakajo A, Che X, Iwashige H, Aridome K, Hokita S, Aikou T (2000) Prognostic value of intratumoral natural killer cells in gastric carcinoma. Cancer 88:577–583
23. Schleypen JS, Baur N, Kammerer R, Nelson PJ, Rohrmann K, Grone EF, Hohenfellner M, Haferkamp A, Pohla H, Schendel DJ, Falk CS, Noessner E (2006) Cytotoxic markers and frequency predict functional capacity of natural killer cells infiltrating renal cell carcinoma. Clin Cancer Res 12:718–725
24. Hanna J, Bechtel P, Zhai Y, Youssef F, McLachlan K, Mandelboim O (2004) Novel insights on human NK cells' immunological modalities revealed by gene expression profiling. J Immunol 173: 6547–6563
25. Ng CJ, Wadleigh DJ, Gangopadhyay A, Hama S, Grijalva VR, Navab M, Fogelman AM, Reddy ST (2001) Paraoxonase-2 is a ubiquitously expressed protein with antioxidant properties and is capable of preventing cell-mediated oxidative modification of low density lipoprotein. J Biol Chem 276:44444–44449
26. Liu H, Zheng F, Cao Q, Ren B, Zhu L, Striker G, Vlassara H (2006) Amelioration of oxidant stress by the defensin lysozyme. Am J Physiol Endocrinol Metab 290:E824–E832
27. MacMicking J, Xie QW, Nathan C (1997) Nitric oxide and macrophage function. Annu Rev Immunol 15:323–350
28. Ohshima H, Tatemichi M, Sawa T (2003) Chemical basis of inflammation-induced carcinogenesis. Arch Biochem Biophys 417:3–11
29. Szatrowski TP, Nathan CF (1991) Production of large amounts of hydrogen peroxide by human tumor cells. Cancer Res 51:794–798
30. Brar SS, Kennedy TP, Sturrock AB, Huecksteadt TP, Quinn MT, Whorton AR, Hoidal JR (2002) An NAD(P)H oxidase regulates growth and transcription in melanoma cells. Am J Physiol Cell Physiol 282:C1212–C1224
31. De Marzo AM, Platz EA, Sutcliffe S, Xu J, Gronberg H, Drake CG, Nakai Y, Isaacs WB, Nelson WG (2007) Inflammation in prostate carcinogenesis. Nat Rev Cancer 7:256–269
32. Van den Hove LE, Van Gool SW, Van Poppel H, Baert L, Coorevits L, Van Damme B, Ceuppens JL (1997) Phenotype, cytokine production and cytolytic capacity of fresh (uncultured) tumour-infiltrating T lymphocytes in human renal cell carcinoma. Clin Exp Immunol 109:501–509
33. Matsuda M, Petersson M, Lenkei R, Taupin JL, Magnusson I, Mellstedt H, Anderson P, Kiessling R (1995) Alterations in the signal-transducing molecules of T cells and NK cells in colorectal tumor-infiltrating, gut mucosal and peripheral lymphocytes: correlation with the stage of the disease. Int J Cancer 61:765–772
34. Ino K, Yamamoto E, Shibata K, Kajiyama H, Yoshida N, Terauchi M, Nawa A, Nagasaka T, Takikawa O, Kikkawa F (2008) Inverse correlation between tumoral indoleamine 2,3-dioxygenase expression and tumor-infiltrating lymphocytes in endometrial cancer: its association with disease progression and survival. Clin Cancer Res 14:2310–2317
35. Devadas S, Zaritskaya L, Rhee SG, Oberley L, Williams MS (2002) Discrete generation of superoxide and hydrogen peroxide by T cell receptor stimulation: selective regulation of mitogen-activated protein kinase activation and fas ligand expression. J Exp Med 195:59–70
36. Williams MS, Kwon J (2004) T cell receptor stimulation, reactive oxygen species, and cell signaling. Free Radic Biol Med 37: 1144–1151